COMMUN. MATH. SCI.
Vol. 11, No. 2, pp. 635–649
© 2013 International Press

FAST COMMUNICATION

A FAST ALGORITHM FOR REITERATED HOMOGENIZATION*

BJÖRN ENGQUIST† AND LEXING YING‡

Abstract. This paper considers the numerical evaluation of effective coefficients for multiscale homogenization problems and proposes a highly efficient algorithm for a certain class of reiterated homogenization problems of practical importance. The main idea of the proposed approach is to introduce a novel object called the homogenization map, approximate it through adaptive interpolation, and replace solutions of the cell problems with fast evaluations of the interpolant. Numerical results are provided for both 2D and 3D problems to demonstrate the efficiency and accuracy of the proposed algorithm.

Key words. Reiterated homogenization, upscaling, effective coefficients, homogenization map, fast algorithms, adaptive sampling.

AMS subject classifications. 35B27, 65K10, 65Y20.

1. Introduction

Homogenization is the theory of deriving effective models for problems with complex structures and oscillatory coefficients. It is a well-studied field with a vast amount of literature; some classical references include [4, 22, 28, 30]. The simplest example of homogenization is probably the following linear elliptic partial differential equation (PDE):

$$\begin{cases} -\mathrm{div}(A(x/\varepsilon)\nabla u(x)^{\varepsilon}) = f(x), & x\in\Omega, \\ u(x) = 0, & x\in\partial\Omega, \end{cases} \tag{1.1}$$

where Ω is a bounded domain in $\mathbb{R}^d$ and the $d\times d$ matrix A is symmetric, positive definite, and periodic in the unit cube $Y=[0,1]^d$. The standard result of the homogenization theory states that $u^{\varepsilon}\to u$ weakly in $H_0^1(\Omega)$ as $\varepsilon\to 0$ and the limit $u(x)$ satisfies the equation

$$\begin{cases} -\mathrm{div}(\bar{A}\nabla u(x)) = f(x), & x\in\Omega, \\ u(x) = 0, & x\in\partial\Omega, \end{cases} \tag{1.2}$$

where the homogenized coefficients $\bar{A}=(\bar{A}_{ij})_{1\le i,j\le d}$ are given by

$$\bar{A}_{ij} = \int_Y (\nabla w_i(y)+e_i)^T A(y)(\nabla w_j(y)+e_j)dy.$$

Here e_i is the unit vector with one at the i-th entry and zero elsewhere, and the corrector function w_i satisfies the cell problem

$$-\mathrm{div}(A(y)(\nabla w_i(y)+e_i)) = 0, \quad y\in Y$$

*Received: July 10, 2012; accepted: August 28, 2012. Communicated by Weinan E.

†Department of Mathematics and ICES, The University of Texas at Austin, 1 University Station C1200, Austin, TX 78712, USA (engquist@math.utexas.edu).

‡Department of Mathematics and ICES, The University of Texas at Austin, 1 University Station C1200, Austin, TX 78712, USA (lexing@math.utexas.edu).

with periodic boundary conditions in the weak sense.

A natural extension of the above problem is so-called reiterated homogenization. This problem, as well as the more general nonlinear cases, have been studied in [6, 7, 24, 25, 26]. A nice review of this topic can be found in [27]. In the simplest linear elliptic PDE setting, the reiterated homogenization studies the problem

$$\begin{cases} -\mathrm{div}(A^\varepsilon(x)\nabla u(x)^\varepsilon) = f(x), & x\in\Omega, \\ u(x) = 0, & x\in\partial\Omega, \end{cases} \tag{1.3}$$

where $A^\varepsilon(x)$ now takes the form

$$A^\varepsilon(x) = A(x, x/\varepsilon, x/\varepsilon^2, \ldots, x/\varepsilon^m).$$

In this case, as $\varepsilon\to 0$, $u^\varepsilon \to u$ weakly in $H_0^1(\Omega)$, with u satisfying

$$\begin{cases} -\mathrm{div}(\bar{A}(x)\nabla u(x)) = f(x), & x\in\Omega, \\ u(x) = 0, & x\in\partial\Omega, \end{cases} \tag{1.4}$$

where $\bar{A}(x)$ is defined through the following reiterated procedure: First, at level m (or equivalently scale $1/\varepsilon^m$), one defines $A_m(x_0,\ldots,x_{m-1})$ for each choice of $(x_0,\ldots,x_{m-1})$ with

$$(A_m(x_0,\ldots,x_{m-1}))_{ij} := \int_Y (\nabla w_i(y) + e_i)^T A(x_0,\ldots,x_{m-1},y)(\nabla w_j(y) + e_j)dy, \tag{1.5}$$

where $w_i(y)$ satisfies

$$-\mathrm{div}(A(x_0,\ldots,x_{m-1},y)(\nabla w_i(y) + e_i)) = 0, \quad y\in Y$$

with periodic boundary conditions. Then, at level k (or scale $1/\varepsilon^k$) with $1\le k\le M-1$, one recursively defines $A_k(x_0,\ldots,x_{k-1})$ for each choice of $(x_0,\ldots,x_{k-1})$ with

$$(A_k(x_0,\ldots,x_{k-1}))_{ij} := \int_Y (\nabla w_i(y) + e_i)^T A_{k+1}(x_0,\ldots,x_{k-1},y)(\nabla w_j(y) + e_j)dy, \tag{1.6}$$

where $w_i(y)$ satisfies

$$-\mathrm{div}(A_{k+1}(x_0,\ldots,x_{k-1},y)(\nabla w_i(y) + e_i)) = 0, \quad y\in Y$$

with periodic boundary conditions. Finally, we define $\bar{A}(x) = A_1(x)$.

This paper is concerned with the efficient evaluation of the homogenized coefficients of the reiterated homogenization problems. In fact, the definition of $\bar{A}(x)$ provides a way for computing it. Let us assume that numerically the unit cube Y is discretized with a grid G_n with n points in each dimension for a total size of n^d. Let the cost of solving the discrete system of the elliptic PDE on this n^d grid be $S_d(n)$. At level m, one needs to solve d cell problems for every choice of $(x_0,\ldots,x_{m-1})$ with $x_0,x_1,\ldots,x_{m-1}\in G_n$, and so the naive cost for this level would be $n^{md}\cdot d\cdot S_d(n)$. A similar argument shows that the cost at level k is $n^{kd}\cdot d\cdot S_d(n)$. Clearly the m-th level dominates the rest and so the total naive computational cost is $O(n^{md}\cdot d\cdot S_d(n)) = O(n^{md}\cdot S_d(n))$. This complexity grows rapidly when the number of levels m gets larger, especially for three-dimensional problems ($d=3$).

In this paper, we propose a significantly more efficient method for a wide subclass of reiterated homogenization problems where the coefficients $A^\varepsilon(x)$ take the following form:

$$\begin{cases} A^\varepsilon(x) = A(x, x/\varepsilon, x/\varepsilon^2, \ldots, x/\varepsilon^m), \\ A(x_0, x_1, \ldots, x_m) = a_0(x) \star_1 a_1(x_1) \star_2 \ldots \star_m a_m(x_m), \end{cases} \tag{1.7}$$

where each $a_i(\cdot)$ is a periodic function on the unit cell Y, each $\star_i$ is a standard binary operator, and the evaluation of the last formula is understood to be taken *from left to right*. The methodology behind the approach to be discussed applies to the general case where the functions $a_i(\cdot)$ are matrix-valued. However, in order to illustrate the main idea clearly and to simplify the discussion, we restrict to the case where the functions $a_i(\cdot)$ are scalar-valued. The binary operators $\star_i$ can be fairly general, for example $a \star_i b$ can be $\min(a,b)$, $\max(a,b)$, $a+b$, or $a \cdot b$.

As we shall see in the numerical examples, though (1.7) has a special form, it is able to represent many practical and important reiterated homogenization structures due to the flexibility of the binary operator $\star_i$. For this special form of reiterated homogenization, our method is able to compute the homogenized coefficients in $O(m \cdot S_d(n))$ steps, which is a dramatic improvement from the $O(n^{md} \cdot S_d(n))$ complexity of the naive procedure.

Reiterated homogenization has become a useful way to design and construct multiscale structures with optimal effective conductive and elastic behaviors; many examples of this type were reported in [11, 27, 28]. The method of this paper can be viewed as an initial step in designing efficient computational tools to explore the vast design space of such materials.

Though there has been very little work specifically on the numerical aspect of reiterated homogenization, many numerical methods have been proposed for other types of homogenization problems. When the coefficients are simply periodic functions as in (1.1), one simply solves the cell problems numerically to obtain the homogenized coefficients. Most of the numerical efforts have focused on the case where the coefficients fail to be periodic. Several representative algorithms include wavelet-based numerical homogenization [2, 8, 12, 17], multiscale finite element methods [3, 20, 21], heterogeneous multiscale methods [15], and equation-free techniques [23], and we refer to the review article [18] for more details. Recently, there has been significant progress in two directions: upscaling for problems with no scale-separation [29] and algorithms for certain classes of stochastic homogenization [1, 5]. In practice, the homogenized coefficients only apply when ε goes to zero, while in many engineering problems one is in fact more interested in the small but finite ε regime. Numerical efforts in this direction can be found in [9], for example.

The rest of this paper is organized as follows. Section 2 describes the main idea of the proposed algorithm along with some implementation details. Section 3 provides some numerical examples to illustrate the efficiency and accuracy of the proposed approach, and several future directions are discussed in Section 4.

2. Algorithm description

2.1. Homogenization map. Let us recall that at level m the coefficients $A_m(x_0, \ldots, x_{m-1})$ are defined via

$$(A_m(x_0, \ldots, x_{m-1}))_{ij} = \int_Y (\nabla w_i(y) + e_i)^T A(x_0, \ldots, x_{m-1}, y)(\nabla w_j(y) + e_j) dy, \tag{2.1}$$

where $w_i(y)$ solves the cell problem

$$-\mathrm{div}(A(x_0,\ldots,x_{m-1},y)(\nabla w_i(y)+e_i))=0,\quad y\in Y$$

with periodic boundary conditions. For the special form

$$A(x_0,x_1,\ldots,x_m)=a_0(x_0)\star_1 a_1(x_1)\star_2\ldots\star_m a_m(x_m)$$

considered here, the cell problem takes the form

$$-\mathrm{div}((a_0(x_0)\star_1\ldots\star_{m-1} a_{m-1}(x_{m-1})\star_m a_m(y))(\nabla w_i+e_i))=0,\quad y\in Y, \tag{2.2}$$

where the evaluation of the $\star_k$ operators are understood to be taken from left to right. We observe that, although the coefficients of (2.2) involve the variables $x_0,\ldots,x_{m-1}$, it is a single number $a_0(x_0)\star_1\ldots\star_{m-1} a_{m-1}(x_{m-1})$ that enters the cell problem. Therefore, the key idea is to introduce the *homogenization map* $T_m : R^+\to\mathbb{R}^{d\times d}$ at level m that maps this number to the resulting homogenized coefficients. More precisely, for a fixed $c\in R^+$, the matrix $T(c)$ is defined by

$$(T_m(c))_{ij}=\int_Y(\nabla w_i(y)+e_i)^T(c\star_m a_m(y))(\nabla w_j(y)+e_j)dy,$$

where $w_i(y)$ satisfies

$$-\mathrm{div}((c\star_m a_m(y))(\nabla w_i(y)+e_i))=0,\quad y\in Y$$

with periodic boundary conditions. In order to simplify the notation, we denote by $\mathcal{H}[\cdot]$ the operator that maps the coefficient function of the cell problem to the homogenized coefficients. The definition of T_m can then be succinctly written as

$$T_m(c)=\mathcal{H}[c\star_m a_m(\cdot)]. \tag{2.3}$$

As we shall see, one can approximate T_m effectively by evaluating it at a small number of values for c adaptively and then constructing an interpolant. Once the interpolant is available,

$$A_m(x_0,\ldots,x_{m-1})=T_m(a_0(x_0)\star_1\ldots\star_{m-1} a_{m-1}(x_{m-1}))$$

can be approximated efficiently with a simple evaluation of the this interpolant.

At level $m-1$, we have

$$(A_{m-1}(x_0,\ldots,x_{m-2}))_{ij}=\int_Y(\nabla w_i(y)+e_i)^T A_m(x_0,\ldots,x_{m-2},y)(\nabla w_j(y)+e_j)dy,$$

where $w_i(y)$ satisfies

$$-\mathrm{div}(A_m(x_0,\ldots,x_{m-2},y)(\nabla w_i(y)+e_i))=0,\quad y\in Y$$

with periodic boundary conditions. Using the definition of T_m, we see that the last cell problem is

$$-\mathrm{div}(T_m(a_0(x_0)\star_1\ldots\star_{m-1} a_{m-1}(y))(\nabla w_i+e_i))=0.$$

If we construct a homogenization map T_{m-1} at level $m-1$ that maps an offset c to

$$T_{m-1}(c)=\mathcal{H}[T_m(c\star_{m-1} a_{m-1}(\cdot))], \tag{2.4}$$

then we have

$$A_{m-1}(x_0,\ldots,x_{m-2}) = T_{m-1}(a_0(x_0) \star_1 \ldots \star_{m-2} a_{m-2}(x_{m-2})).$$

Similarly if we define the homogenization map T_k at level k through

$$T_k(c) = \mathcal{H}[T_{k+1}(c \star_k a_k(\cdot))], \tag{2.5}$$

then we have

$$A_k(x_0,\ldots,x_{k-1}) = T_k(a_0(x_0) \star_1 \ldots \star_{k-1} a_{k-1}(x_{k-1})).$$

Finally, at level 1, we have

$$A_1(x_0) = T_1(a_0(x_0)). \tag{2.6}$$

and the homogenized coefficients are $\bar{A}(x) = A_1(x) = T_1(a_0(x))$.

Since one only needs to calculate the homogenized coefficients $\bar{A}$, we can then forget about the functions A_k and focus on the homogenization maps $T_k(\cdot)$ and their recurrence relationship ((2.3), (2.4), (2.5), and (2.6)). Computationally, for each map T_{k+1}, we need to evaluate its values at a grid of its parameter space and then form its interpolant that will be used in the definition of the map T_k. This gives rise to the following algorithm for computing the homogenized coefficients.

ALGORITHM 2.1. *Fast computation of reiterated homogenized coefficients.*

1: Construct an interpolant for T_m defined by $T_m(c) = \mathcal{H}[c \star_m a_m(\cdot)]$.
2: **for** $k = m-1,\ldots,1$ **do**
3: Construct an interpolant for T_k defined by $T_k(c) = \mathcal{H}[T_{k+1}(c \star_k a_k(\cdot))]$. The evaluation of $T_{k+1}(\cdot)$ is approximated by evaluating the existing interpolant of $T_{k+1}(\cdot)$.
4: **end for**
5: $\bar{A}(x) = T_1(a_0(x))$.

2.2. Implementation details and complexity analysis. Algorithm 2.1 is conceptually simple, however the implementation details are essential to its accuracy and efficiency. The main reason is that the map $T_k(\cdot)$ is a function with limited smoothness and therefore adaptive sampling is required in the construction of its interpolant. In the following discussion, we assume that $a_k(y) \geq 0$ for each k, which is a reasonable assumption since we consider the coefficients of elliptic PDEs.

The first problem is how to represent the map $T_k : \mathbb{R}^+ \to \mathbb{R}^{d\times d}$. The deciding criterion is that the map T_k should be sufficiently regular in the chosen representation. One naive approach is to construct the interpolant using the offset variable c directly as the parameter. However, the following simple example shows that the homogenization map can have singularity near $c = 0$. Let $a(y)$ be a continuous function defined on the unit cell $[-1/2, 1/2)$ and consider the homogenization map

$$T(c) = \mathcal{H}[c + a(\cdot)],$$

with $+$ as the binary operator. For simplicity, we assume that $a(y)$ has a global minimum equal to zero and reaches its minimum at $y = 0$. When the leading order behavior of $a(y)$ is given by $|y|^m$, an easy calculation shows that

$$T(c) \approx \left(\frac{1}{|y|^m + c}\right)^{-1} \approx (c^{1-1/m}).$$

Therefore, the homogenization map has limited smoothness near $c=0$ even in this simple case. However, if we look at homogenization map in the log-log scale, i.e.,

$$T^{ll}(\alpha) := \log(T(e^{\alpha})),$$

where $\log(\cdot)$ stands for the *matrix logarithm* for symmetric positive definite matrices, this map behaves linearly no matter what m is. Therefore, it is favorable to interpolate each homogenization map $T_k(\cdot)$ in its log-log form $T_k^{ll}(\cdot):\mathbb{R}\to\mathbb{R}^{d\times d}$.

The second problem is that, even represented in the log-log scale, the maps $T_k^{ll}(\cdot)$ often have jumps in their derivatives when the operators $\star_k$ lack smoothness, for example when $\star_k = \min(\cdot,\cdot)$, or $\max(\cdot,\cdot)$. Since the locations of the jumps in the derivatives are unknown a priori or difficult to figure out in advance, any interpolation scheme with fixed grid will certainly result in large interpolation error. Therefore, we adopt the following adaptive piecewise linear interpolation scheme to represent the maps $T_k^{ll}(\cdot):\mathbb{R}\to\mathbb{R}^{d\times d}$. Initially, a rather coarse uniform Cartesian grid of step size h_0 is placed on the interval $[\alpha_L,\alpha_R]$, where α_L and α_R are chosen so that this interval covers all possible locations where the evaluations of the homogenization map can take place. The homogenization map is then evaluated at this uniform grid to form an initial piecewise linear interpolant. Next, we adaptively insert new grid points at locations where the interpolant is not sufficiently accurate, as long as the local step size is above a predetermined threshold $h_{\min}$. In order to decide whether the interpolant is sufficiently accurate at a grid point α_i, we estimate the local jump in the first derivative:

$$J_i := \left\| \frac{f_{i+1}-f_i}{\alpha_{i+1}-\alpha_i} - \frac{f_i-f_{i-1}}{\alpha_i-\alpha_{i-1}} \right\|,$$

where f_{i-1}, f_i, and f_{i+1} are the map values at grids α_{i-1}, α_i, and α_{i+1}. If the map T_k^{ll} is smooth near α_i, then the jump J_i should approach zero as we refine. If J_i is above a predetermined constant $J_{\max}$, we refine the interpolation by inserting two new points at $(\alpha_{i-1}+\alpha_i)/2$ and $(\alpha_i+\alpha_{i+1})/2$, and repeat until no extra grid points can be inserted. This adaptive scheme refines the interpolant automatically near the jump locations (in the derivative) and in practice the resulting interpolant only uses a few dozen grid points as we will see in the numerical examples.

The third problem concerns the numerical solution of the cell problem, i.e., the evaluation of $\mathcal{H}[\cdot]$. Since most interesting homogenization problems involve coefficients with large contrasts and/or sharp discontinuities, the solution of the cell problem needs to be able to address these two situations efficiently. In the current implementation, we discretize the cell problem using spectral element methods [10] with element boundary aligned with the discontinuities in the coefficients. This allows us to approximate the solution of the cell problem efficiently. For the numerical solution of the discrete system, we use the multifrontal method with nested dissection [13, 19] due to its robustness for problems with large contrasts. For each cell problem, the solution cost $S_d(n)$ is $O(n^3)$ in 2D ($d=2$) and $O(n^6)$ in 3D ($d=3$).

Let us now estimate the complexity of the proposed approach. For each level k, the algorithm constructs an interpolant for T_k. As we mentioned earlier, the number of samples required for our adaptive scheme is a moderate constant in practice. For each sample, one needs to solve a cell problem, which takes $O(S_d(n))$ steps. Putting these numbers together, we conclude that the overall complexity of the proposed approach is $O(m\cdot S_d(n))$, which is a drastic improvement over the $O(n^{md}\cdot S_d(n))$ cost of the naive approach mentioned in Section 1.

3. Numerical results

In this section, we provide some numerical examples to demonstrate the efficiency and accuracy of the proposed method. All numerical results are obtained on a desktop with a 2.8GHz CPU. The predetermined constants $h_{\min}$ and $J_{\max}$ in the adaptive interpolation scheme are set to be 10^{-3} and 10^{-2}, respectively.

3.1. 2D problems.

Example 1. We start with a problem with $m=3$. At each level $k=1,2,3$, the coefficient function is given by

$$a_k(y_1,y_2)=\begin{cases}1, & \max(|y_1-1/2|,|y_2-1/2|)\geq 1/4,\\ 0.1, & \text{otherwise,}\end{cases}$$

and $\star_k$ is equal to $\min(\cdot,\cdot)$ at all levels. An example of $A^\varepsilon(x)$ with $\varepsilon=1/4$ is given in figure 3.1. At each level, the homogenization map $T_k(\cdot)$ is represented in the log-log scale with the adaptive interpolant discussed above. The number of samples and the construction cost (in seconds) of the interpolants at all levels are listed in table 3.1. Notice that at each level the number of samples remains moderate and the construction time is around one second.

Figure 3.2 plots the homogenization map $T_1(\cdot)$ in the log-log scale. Due to the limited smoothness of $\min(\cdot,\cdot)$, the homogenization map exhibits jumps in its derivatives at several locations and the adaptive interpolation scheme automatically refines near them. Once the map T_1 is available, we compute the homogenized coefficients for three test cases $a_0(x)=0.1$, 0.5, and 1. The resulting $\bar{A}$ is equal to

$$\begin{pmatrix}0.1000 & 0\\ 0 & 0.1000\end{pmatrix},\qquad \begin{pmatrix}0.2108 & 0\\ 0 & 0.2108\end{pmatrix},\qquad \begin{pmatrix}0.3186 & 0\\ 0 & 0.3186\end{pmatrix},$$

respectively. Notice that when $a_0(x)=0.1$ the problem reduces to $A(x_0,x_1,\ldots,x_m)=0.1$ and hence the result by the proposed algorithm is exact.

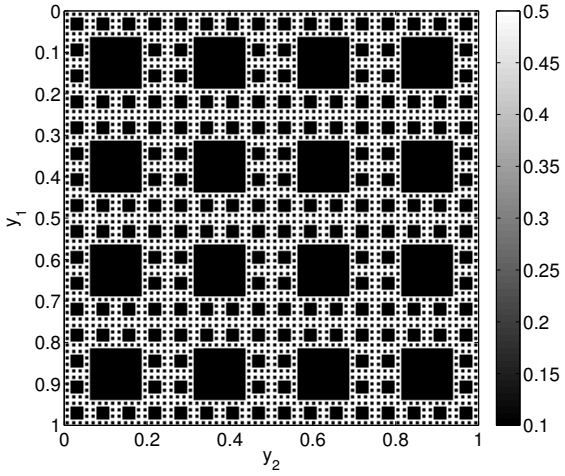

FIG. 3.1. *Example 1. The coefficients $A^\varepsilon(x)$ for $\varepsilon=1/4$.*

In many applications, the actual period of the coefficient function is not known exactly (or even worse, the coefficients fail to be periodic). One way to get around

TABLE 3.1. *Example 1. The number of samples at each level and the interpolant construction time in seconds.*

k	No. of samples	Construction time(s)
3	86	1.1e+00
2	89	1.3e+00
1	92	1.3e+00

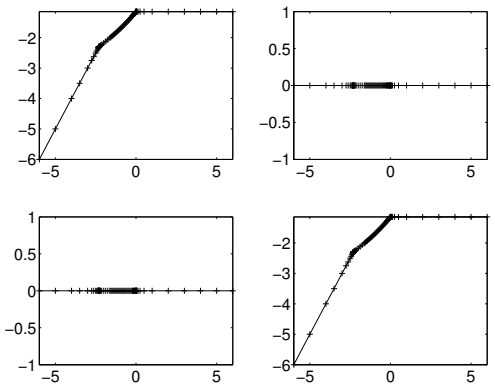

FIG. 3.2. *Example 1. The homogenization map $T_1(\cdot)$ plotted in the log-log form $T_1^{ll}(\cdot)$. Each subplot shows a single component.*

this is to solve the cell problem with an arbitrary size δ that is significantly larger than the actual period. It has been shown (for example in [16]) that the result of this inaccurate cell problem converges to the correct homogenized coefficients as the ratio of the actual period over δ goes to zero. In practice, this convergence takes place fairly rapidly as long as the ratio is sufficiently small (see [14] for example). To study how the proposed algorithm behaves in this situation, we repeat the above calculation, but with the cell size δ set to be 2.5 times the actual period. The resulting $\bar{A}$ calculated with this inaccurate period is given by

$$\begin{pmatrix} 0.1000 & 0 \\ 0 & 0.1000 \end{pmatrix}, \qquad \begin{pmatrix} 0.2109 & 0 \\ 0 & 0.2109 \end{pmatrix}, \qquad \begin{pmatrix} 0.3187 & 0 \\ 0 & 0.3187 \end{pmatrix}$$

for $a_0(x) = 0.1,\ 0.5,\ 1$, respectively. Notice that there is only a slight difference between these numbers and the correct values given above. This demonstrates that the proposed algorithm shares this robustness and provides good approximations for the reiterated homogenization coefficients even if the period is unknown.

Example 2. This problem again has $m = 3$. The coefficient functions are given by

$$a_1(y_1, y_2) = a_3(y_1, y_2) = \begin{cases} 1, & |y_1 - 1/2| \geq 1/4, \\ 0.1, & \text{otherwise} \end{cases}$$

and

$$a_2(y_1, y_2) = \begin{cases} 1, & |y_2 - 1/2| \geq 1/4, \\ 0.1, & \text{otherwise.} \end{cases}$$

The $\star_k$ operators are all equal to $\min(\cdot,\cdot)$. An example of $A^\varepsilon(x)$ with $\varepsilon = 1/4$ is given in figure 3.3. The number of samples and the construction cost (in seconds) of the interpolant at each level are listed in table 3.2.

Figure 3.4 plots the homogenization map $T_1(\cdot)$ in the log-log scale. Once the map T_1 is available, the homogenized coefficients are evaluated for three test cases $a_0(x) = 0.1, 0.5, 1$. The resulting coefficients $\bar{A}$ are given by

$$\begin{pmatrix} 0.1000 & 0 \\ 0 & 0.1000 \end{pmatrix}, \qquad \begin{pmatrix} 0.1143 & 0 \\ 0 & 0.1250 \end{pmatrix}, \qquad \begin{pmatrix} 0.1170 & 0 \\ 0 & 0.1346 \end{pmatrix},$$

respectively.

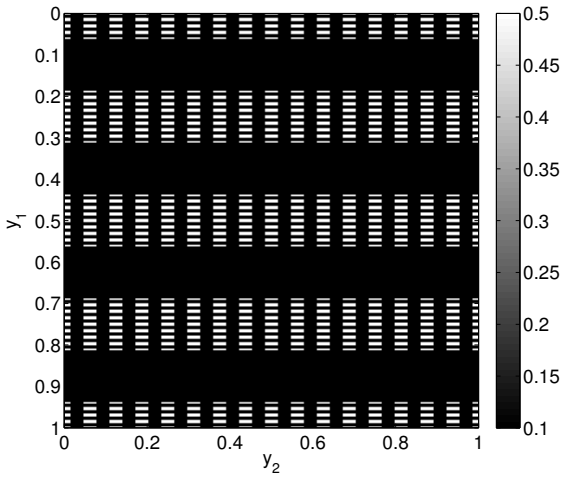

FIG. 3.3. *Example 2. The coefficients $A^\varepsilon(x)$ for $\varepsilon = 1/4$.*

TABLE 3.2. *Example 2. The number of samples at each level and the interpolant construction time in seconds.*

k	No. of samples	Construction time(s)
3	114	1.6e+00
2	114	1.6e+00
1	114	1.6e+00

3.2. 3D problems.

Example 3. Here we choose $m = 4$. The coefficient functions $a_k(y)$ at all levels are given by

$$a_k(y_1, y_2, y_3) = \begin{cases} 1, & \max(|y_1 - 1/2|, |y_2 - 1/2|, |y_3 - 1/2|) \geq 1/4, \\ 0.1, & \text{otherwise}, \end{cases}$$

and $\star_k$ is the $\min(\cdot,\cdot)$ function at all levels. The number of samples and the construction cost (in seconds) of the interpolant at each level are listed in table 3.3.

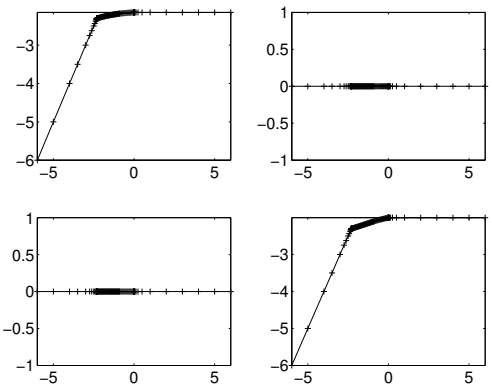

FIG. 3.4. *Example 2. The homogenization map $T_1(\cdot)$ plotted in the log-log form $T_1^{ll}(\cdot)$. Each subplot shows a single component.*

Figure 3.5 plots the homogenization map $T_1(\cdot)$ in the log-log scale. Once the map T_1 is available, the homogenized coefficients are calculated for three test cases $a_0(x) = 0.1, 0.5, 1$. The coefficients $\bar{A}$ are equal to

$$\begin{pmatrix} 0.1000 & 0 & 0 \\ 0 & 0.1000 & 0 \\ 0 & 0 & 0.1000 \end{pmatrix}, \quad \begin{pmatrix} 0.2951 & 0 & 0 \\ 0 & 0.2951 & 0 \\ 0 & 0 & 0.2951 \end{pmatrix}, \quad \begin{pmatrix} 0.5180 & 0 & 0 \\ 0 & 0.5180 & 0 \\ 0 & 0 & 0.5180 \end{pmatrix},$$

respectively.

TABLE 3.3. *Example 3. The number of samples at each level and the interpolant construction time in seconds.*

k	No. of samples	Construction time(s)
4	70	5.1e+01
3	86	6.1e+01
2	97	6.9e+01
1	111	7.9e+01

Example 4. This example has $m = 4$ as well. The coefficient functions $a_k(y)$ are given by

$$a_1(y_1, y_2, y_3) = a_4(y_1, y_2, y_3) = \begin{cases} 1, & |y_1 - 1/2| \geq 1/4, \\ 0.1, & \text{otherwise}, \end{cases}$$

$$a_2(y_1, y_2, y_3) = \begin{cases} 1, & |y_2 - 1/2| \geq 1/4, \\ 0.1, & \text{otherwise}, \end{cases}$$

and

$$a_3(y_1, y_2, y_3) = \begin{cases} 1, & |y_3 - 1/2| \geq 1/4, \\ 0.1, & \text{otherwise}. \end{cases}$$

The $\star_k$ operators are all $\min(\cdot, \cdot)$. The number of samples and the construction cost (in seconds) of the interpolant at each level are listed in table 3.4.

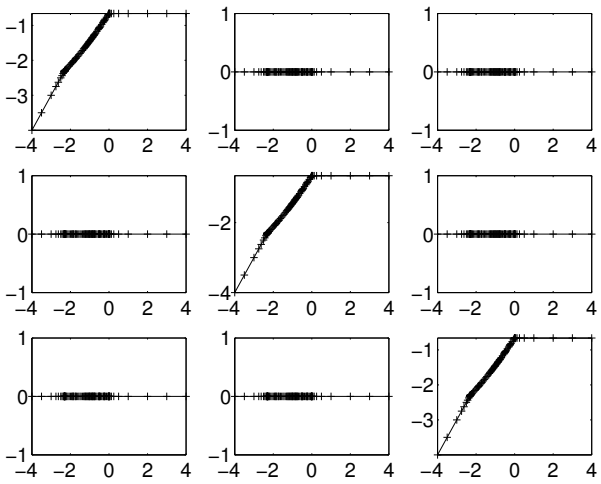

FIG. 3.5. *Example 3. The homogenization map $T_1(\cdot)$ plotted in the log-log form $T_1^{ll}(\cdot)$. Each subplot shows a single component.*

Figure 3.6 plots the homogenization map $T_1(\cdot)$ in the log-log scale. Once the map T_1 is available, the homogenized coefficients are calculated for three test cases $a_0(x) = 0.1, 0.5, 1$. The coefficients $\bar{A}$ in these three cases are equal to

$$\begin{pmatrix} 0.1000 & 0 & 0 \\ 0 & 0.1000 & 0 \\ 0 & 0 & 0.1000 \end{pmatrix}, \quad \begin{pmatrix} 0.1077 & 0 & 0 \\ 0 & 0.1167 & 0 \\ 0 & 0 & 0.1125 \end{pmatrix}, \quad \begin{pmatrix} 0.1093 & 0 & 0 \\ 0 & 0.1265 & 0 \\ 0 & 0 & 0.1173 \end{pmatrix},$$

respectively.

TABLE 3.4. *Example 4. The number of samples at each level and the interpolant construction time in seconds.*

k	No. of samples	Construction time(s)
4	110	7.7e+01
3	134	9.8e+01
2	134	1.0e+02
1	134	1.0e+02

3.3. Convergence in ε. We now study how the finite-ε problem approaches the homogenization limit as ε goes to zero. To do that, we vary the parameter ε, form the coefficients $A^\varepsilon(x)$ following (1.7) for each value of ε, and calculate the finite-ε effective coefficients $\bar{A}^\varepsilon$ by solving the cell problem

$$(\bar{A}^\varepsilon)_{ij} := \int_Y (\nabla w_i(y) + e_i)^T A^\varepsilon(y)(\nabla w_j(y) + e_i) dy, \tag{3.1}$$

where $w_i(y)$ satisfies

$$-\mathrm{div}(A^\varepsilon(y)(\nabla w_i(y) + e_i)) = 0, \quad y \in Y$$

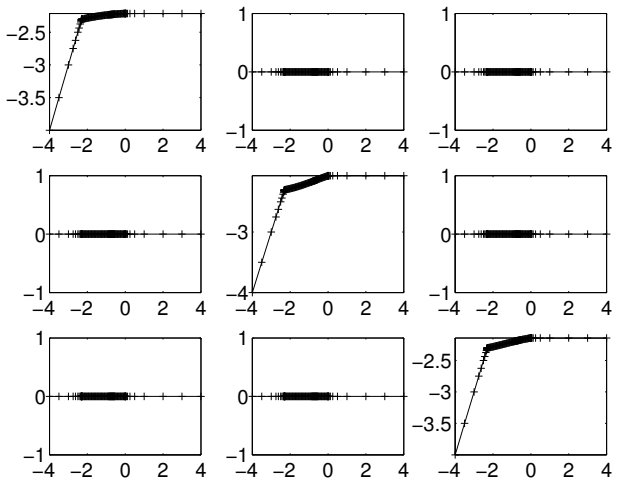

FIG. 3.6. *Example 4. The homogenization map $T_1(\cdot)$ plotted in the log-log form $T_1^{ll}(\cdot)$. Each subplot shows a single component.*

with periodic boundary conditions. When either the dimension d or the number of levels m is large, the full representation of the coefficient matrix $A^\varepsilon(x)$ quickly exhausts the memory space as ε decreases. Therefore, we restrict our numerical tests to the 2D case ($d=2$) with $m=2$.

Example 5. In this test, the coefficient functions are given by

$$a_k(y_1,y_2)=\begin{cases}1, & \max(|y_1-1/2|,|y_2-1/2|)\geq 1/4,\\ 0.1, & \text{otherwise},\end{cases}$$

for $k=1,2$ and the binary operators $\star_k$ are the $\min(\cdot,\cdot)$ function at all levels. We pick $a_0(x)=0.5$, and the limiting homogenized coefficients $\bar{A}$ are equal to

$$\begin{pmatrix}0.2666 & 0\\ 0 & 0.2666\end{pmatrix}.$$

The finite-ε effective coefficients are computed for $1/\varepsilon=2,3,\ldots,8$, and the difference $\|\bar{A}^\varepsilon-\bar{A}\|$ is plotted in figure 3.7. We see clearly that as ε approaches zero the finite-ε effective coefficients approach the homogenized coefficients computed by our algorithm.

Example 6. In this example, the coefficient functions are

$$a_1(y_1,y_2)=\begin{cases}1, & |y_1-1/2|\geq 1/4,\\ 0.1, & \text{otherwise}\end{cases}$$

and

$$a_2(y_1,y_2)=\begin{cases}1, & |y_2-1/2|\geq 1/4,\\ 0.1, & \text{otherwise}.\end{cases}$$

The binary operators $\star_k$ are again the $\min(\cdot,\cdot)$ function at all levels. We choose $a_0(x)=0.5$, and the homogenized coefficients $\bar{A}$ are equal to

$$\begin{pmatrix}0.1496 & 0\\ 0 & 0.1330\end{pmatrix}.$$

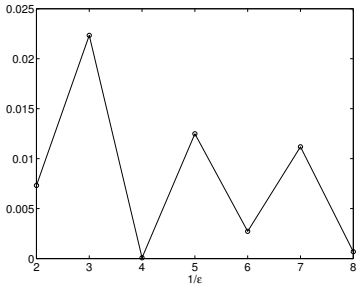

FIG. 3.7. *Example 5. Convergence of the finite-ε effective coefficients $\bar{A}^\varepsilon$ to the homogenized coefficients $\bar{A}$ as ε goes to zero.*

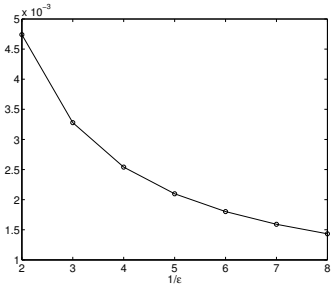

FIG. 3.8. *Example 6. Convergence of the finite-ε effective coefficients $\bar{A}^\varepsilon$ to the homogenized coefficients $\bar{A}$ as ε goes to zero.*

The finite-ε effective coefficients are computed for $1/\varepsilon = 2,3,\ldots,8$, and the difference between $\bar{A}^\varepsilon$ and $\bar{A}$ is plotted in figure 3.8.

4. Conclusions and future work

This paper describes an efficient algorithm for computing the homogenized coefficients for a certain class of linear reiterated homogenization problems. The essential idea is to introduce a novel object called the homogenization map, approximate it through adaptive interpolation, and replace expensive solutions of cell problems with fast evaluations of the interpolant. The resulting algorithm is accurate and provides a drastic speedup over the naive algorithm. Numerical results are provided in both 2D and 3D for practical examples.

There are several directions for future work. First, the methodology clearly extends to the nonlinear homogenization problems discussed in [6, 7, 24, 25, 26]. Second, the component functions $a_i(y)$ considered here are scalar functions, and a slightly more general case is that of matrix-valued component functions, as we already mentioned. Third, we have so far only considered scalar elliptic problems in the divergence form, and it would be of practical interest to consider homogenization for Maxwell's equations and also systems of linear elasticity. Finally, the idea behind the homogenization map can also be applied to numerical averaging of multiscale dynamical systems [30].

Acknowledgment. B.E. is partially supported by NSF grant DMS-1027952. L.Y. is partially supported by NSF CAREER grant DMS-0846501 and NSF grant DMS-1027952. The authors thank Jack Poulson for providing suggestions and comments.

REFERENCES

[1] A. Anantharaman and C. Le Bris, *A numerical approach related to defect-type theories for some weakly random problems in homogenization*, Multiscale Model. Simul., 9(2), 513–544, 2011.

[2] U. Andersson, B. Engquist, G. Ledfelt, and O. Runborg, *A contribution to wavelet-based subgrid modeling*, Appl. Comput. Harmon. Anal., 7(2), 151–164, 1999.

[3] I. Babuška, G. Caloz, and J.E. Osborn, *Special finite element methods for a class of second order elliptic problems with rough coefficients*, SIAM J. Numer. Anal., 31(4), 945–981, 1994.

[4] A. Bensoussan, J.L. Lions, and G. Papanicolaou, *Asymptotic Analysis for Periodic Structures*, AMS Chelsea Publishing, Providence, RI, 2011. Corrected reprint of the 1978 original [MR0503330].

[5] X. Blanc, C. Le Bris, and P.-L. Lions, *Stochastic homogenization and random lattices*, J. Math. Pures Appl. (9), 88(1), 34–63, 2007.

[6] A. Braides and A. Defranceschi, *Homogenization of Multiple Integrals*, in Oxford Lecture Series in Mathematics and its Applications, The Clarendon Press Oxford University Press, New York, 12, 1998.

[7] A. Braides and D. Lukkassen, *Reiterated homogenization of integral functionals*, Math. Models Methods Appl. Sci., 10(1), 47–71, 2000.

[8] M.E. Brewster and G. Beylkin, *A multiresolution strategy for numerical homogenization*, Appl. Comput. Harmon. Anal., 2(4), 327–349, 1995.

[9] J. Byström, J. Helsing, and A. Meidell, *Some computational aspects of iterated structures*, Composites Part B: Engineering, 32(6), 485–490, 2001.

[10] C. Canuto, M.Y. Hussaini, A. Quarteroni, and T.A. Zang, *Spectral Methods in Fluid Dynamics*, Springer Series in Computational Physics, Springer-Verlag, New York, 1988.

[11] A. Cherkaev and R. Kohn (eds.), *Topics in the Mathematical Modelling of Composite Materials*, Progress in Nonlinear Differential Equations and their Applications, 31. Birkhäuser Boston Inc., Boston, MA, 1997.

[12] M. Dorobantu and B. Engquist, *Wavelet-based numerical homogenization*, SIAM J. Numer. Anal., 35(2), 540–559 (electronic), 1998.

[13] I.S. Duff and J.K. Reid, *The multifrontal solution of indefinite sparse symmetric linear equations*, ACM Trans. Math. Software, 9(3), 302–325, 1983.

[14] L.J. Durlofsky, *Upscaling and gridding of fine scale geological models for flow simulation*, in Proceedings of the 8th International Forum on Reservoir Simulation, Stresa, Italy, June 20-25, 2005.

[15] W. E and B. Engquist, *The heterogeneous multiscale methods*, Comm. Math. Sci., 1(1), 87–132, 2003.

[16] W. E, P. Ming, and P. Zhang, *Analysis of the heterogeneous multiscale method for elliptic homogenization problems*, J. Amer. Math. Soc., 18(1), 121–156 (electronic), 2005.

[17] B. Engquist and O. Runborg, *Wavelet-based numerical homogenization with applications*, in Multiscale and Multiresolution Methods, Lect. Notes Comput. Sci. Eng., Springer, Berlin, 20, 97–148, 2002.

[18] B. Engquist and P.E. Souganidis, *Asymptotic and numerical homogenization*, Acta Numer., 17, 147–190, 2008.

[19] A. George, *Nested dissection of a regular finite element mesh*, SIAM J. Numer. Anal., 10, 345–363, 1973.

[20] T.Y. Hou, *Numerical approximations to multiscale solutions in partial differential equations*, in Frontiers in Numerical Analysis (Durham, 2002), Universitext, Springer, Berlin, 241–301, 2003.

[21] T.Y. Hou and X.H. Wu, *A multiscale finite element method for elliptic problems in composite materials and porous media*, J. Comput. Phys., 134(1), 169–189, 1997.

[22] V.V. Jikov, S.M. Kozlov, and O.A. Oleinik, *Homogenization of Differential Operators and Integral Functionals*, Springer-Verlag, Berlin, 1994.

[23] I.G. Kevrekidis, C.W. Gear, J.M. Hyman, P.G. Kevrekidis, O. Runborg, and C. Theodoropoulos, *Equation-free, coarse-grained multiscale computation: Enabling microscopic simulators to perform system-level analysis*, Comm. Math. Sci., 1(4), 715–762, 2003.

[24] J.L. Lions, D. Lukkassen, L.E. Persson, and P. Wall, *Reiterated homogenization of monotone operators*, C.R. Acad. Sci. Paris Sér. I Math., 330(8), 675–680, 2000.

[25] J.L. Lions, D. Lukkassen, L.E. Persson, and P. Wall, *Reiterated homogenization of nonlinear monotone operators*, Chinese Ann. Math. Ser. B, 22(1), 1–12, 2001.

[26] D. Lukkassen, *Reiterated homogenization of non-standard Lagrangians*, C.R. Acad. Sci. Paris Sér. I Math., 332(11), 999–1004, 2001.

[27] D. Lukkassen and G.W. Milton, *On hierarchical structures and reiterated homogenization*, in Function Spaces, Interpolation Theory and Related Topics (Lund, 2000), de Gruyter, Berlin, 355–368, 2002.
[28] G.W. Milton, *The Theory of Composites*, Cambridge Monographs on Applied and Computational Mathematics, Cambridge University Press, Cambridge, 6, 2002.
[29] H. Owhadi and L. Zhang, *Metric-based upscaling*, Comm. Pure Appl. Math., 60(5), 675–723, 2007.
[30] G.A. Pavliotis and A.M. Stuart, *Multiscale Methods*, Texts in Applied Mathematics, Springer, New York, Averaging and Homogenization 53, 2008.